Effect of Oxygen and Temperature on Thermal Decomposition Characteristics of C_4F_7N/CO_2/O_2 Gas Mixture for MV Equipment

FANCHAO YE[1], XIAOXING ZHANG[1,2], CHENG XIE[3], (Member, IEEE), XIANG SUN[3], PENG WU[1], SONG XIAO[1], (Member, IEEE), JU TANG[1], (Member, IEEE), AND YI LI[1], (Graduate Student Member, IEEE)

[1]School of Electrical Engineering and Automation, Wuhan University, Wuhan 430072, China
[2]Hubei Key Laboratory for High-efficiency Utilization of Solar Energy and Operation Control of Energy Storage System, Hubei University of Technology, Wuhan 430068, China
[3]State Grid Zhejiang Electric Power Research Institute, Hangzhou 310007, China

Corresponding authors: Xiaoxing Zhang (xiaoxing.zhang@outlook.com) and Yi Li (liyi_whuee@163.com)

ABSTRACT Perfluoroisobutyronitrile (C_4F_7N)/CO_2/O_2 has been considered as a potential eco-friendly gas insulating medium to replace SF_6 due to its unique dielectric properties. Nowadays, few studies on the thermal stability and decomposition properties of C_4F_7N/CO_2/O_2 gas mixture were reported, which needs to be evaluated comprehensively. Herein, for the first time, we explored the effect of oxygen and temperature on thermal decomposition characteristics of C_4F_7N/CO_2/O_2 gas mixture. It was found that CF_4, C_3F_8, C_3F_6, CO, COF_2, CF_3CN, C_2F_5CN and C_2N_2 are the main by-products of C_4F_7N/CO_2/O_2 gas mixture upon decomposition. The addition of 2%-10% O_2 in the C_4F_7N/CO_2 gas mixture yielded decreased of C_3F_6 and C_2N_2 while the increase of other by-products. The yields and effective formation rates of C_3F_8 and COF_2 accelerated when the content of O_2 was higher than 8%. In terms of practical application, adding 4-6% O_2 to C_4F_7N/CO_2 gas mixture is appropriate and COF_2, C_2N_2, C_2F_5CN can be used as the characteristic products to reflect the severity of partial overheating fault of C_4F_7N/CO_2/O_2 gas insulated equipment.

INDEX TERMS C_4F_7N/CO_2/O_2, partial overheating fault, decomposition characteristic, SF_6 alternative gas, MV equipment.

I. INTRODUCTION

Sulfur hexafluoride (SF_6) has been widely applied in the power industry considering its excellent arc extinguishing and insulation properties, such as gas-insulated switchgear (GIS) and gas-insulated line (GIL) [1]. However, SF_6 is an extremely strong greenhouse gas with high global warming potential (GWP, 23500) and long atmospheric lifetime (3200 years), this will influence global warming seriously at a long time [2], [3]. Seeking for the eco-friendly gas-insulating medium to replace SF_6 employed in gas-insulated equipment (GIE) have become a hot topic now [4], [5].

Recently, Perfluoroisobutyronitrile (C_4F_7N) gas mixture was introduced as eco-friendly gas-insulating medium to replace SF_6 using in GIE. Perfluoroisobutyronitrile (C_4F_7N)

has the GWP of 2100, dielectric strength twice that of pure SF_6 and the boiling point of $-4.7°C$ [6], [7]. CO_2 has been selected as the bugger gas for C_4F_7N due to its significant arc extinguishing performance, exhibiting strong synergy with C_4F_7N [8]. The GWP of C_4F_7N/CO_2 gas mixture containing 4%, 6% C_4F_7N are 327 and 462 respectively, which is 98% less than that of SF_6 [7]. As for engineering application, a 420kV C_4F_7N/CO_2 GIL using and 145kV C_4F_7N/CO_2 GIS have been put into trial operation [9].

For GIS application, it was reported that O_2 should be added to the C_4F_7N/CO_2 gas mixture as the second additive gas to improve the switching performance and reduce the generation of harmful solid by-products (carbon particles) [10], [11]. The influence of O_2 addition on the thermal stability of C_4F_7N gas mixture must be re-evaluated considering the strong oxidizing properties of O_2 for long term application period although the above advantages occur during engineering applications [12]. At present, there are few

The associate editor coordinating the review of this manuscript and approving it for publication was Derek Abbott.

reports on the effect mechanism of O_2 on the thermal stability and decomposition characteristics of $C_4F_7N/CO_2/O_2$ gas mixture.

In addition, when GIE possesses defects such as poor contact, magnetic saturation effect or overloading, the thermal stability of the defective part will be destroyed, which will cause partial overheating fault (POF) [1]. On one hand, the degradation can be accelerated at the presence of POF, even damaging the insulating material and causing partial discharge (PD) or insulation breakdown. On the other hand, POF also induces decomposition of gas insulating medium to generate various by-products. For example, several by-products such as H_2S, SO_2, SOF_2, SO_2F_2 can be found to be used as operation state assessment components for GIE with SF_6 as insulating medium [13]. GIE with C_4F_7N gas mixture as insulating medium can also be monitored and diagnosed by detecting the characteristic decomposition products. Although the influence regularity of O_2 on dielectric and discharge decomposition properties of C_4F_7N-CO_2-O_2 gas mixture has been revealed [12], the reaction mechanism of gas mixture is different under discharge and POF condition considering the unequal energy release amount and duration time. Our group has investigated the effect of temperature and pressure on the thermal decomposition characteristics of C_4F_7N/CO_2 gas mixture [14], while there are still few studies focusing on the effect of O_2 on the POF decomposition properties of $C_4F_7N/CO_2/O_2$ gas mixture.

In this article, we explored the thermal stability and POF decomposition characteristics of $C_4F_7N/CO_2/O_2$ gas mixture. The effect mechanism of oxygen and temperature on the POF decomposition characteristics of $C_4F_7N/CO_2/O_2$ gas mixture was revealed. And the optimal O_2 addition ratio was also obtained. Related research results not only revealed the thermal stability of $C_4F_7N/CO_2/O_2$ gas mixture, but also provides guidance for diagnosis of POF in $C_4F_7N/CO_2/O_2$ GIE.

II. EXPERIMENTAL SETUP AND MEASUREMENT
A. THE POF DECOMPOSITION TEST PLATFORM SETUP
The POF decomposition platform shown in Figure 1 mainly includes sealed stainless-steel gas chamber, switching power supply, POF physical defect model (heating element), temperature sensor, temperature controller, solid-state relay and barometer. The heating element is used to simulate partial overheating inside the GIE located in the center of the stainless-steel gas chamber. The switching power supply provides low-voltage DC power (24V, 120W) to the heating element. The temperature control system is composed of temperature sensor and solid-state relay, meanwhile proportional-integral-derivative (PID) method is adopted. The working temperature of the heating element is measured using the temperature sensor (K-type thermocouple) and the PID control link compares the set value with the feedback signal, then outputs a trigger pulse signal to the solid-state relay according to the calculation result. The no-deviating regulation between the working temperature and the set value is achieved in this system. The stainless-steel gas chamber (10L) is made of 304L stainless steel, which could withstand a pressure of 0.7MPa.
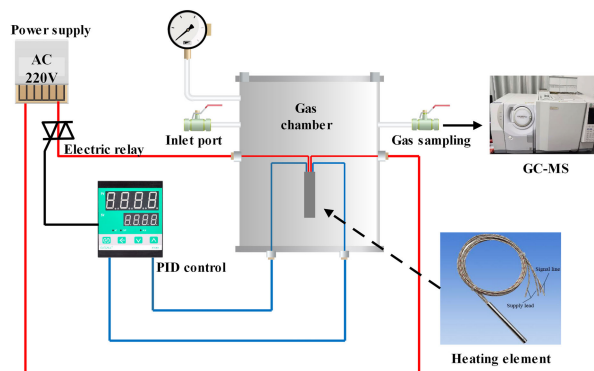

FIGURE 1. The schematic diagram of local overheating decomposition test platform.

TABLE 1. Separation Conditions in Gas Chromatograph.

Chromatograph condition	Parameter setting
Oven	32°C hold for 9 min
	60°C/min to 150°C
	hold for 2 min
Injection port temperature	200°C
Ion source temperature	200°C
Split ratio	10:1

B. POF DECOMPOSITION PRODUCTS DETECTION SYSTEM
Gas chromatography-mass spectrometry (GC-MS, QP2010 Ultra) was used to examine the decomposition products of C_4F_7N-CO_2-O_2 gas mixture (as shown in Fig. 1). The column model is CP-Sil5CB (60m $*$ 8um $*$ 0.32mm), which can effectively separate CF_4, C_2F_6, C_3F_6, C_3F_8, CO, CF_3CN, C_2F_5CN, COF_2, $(CN)_2$. The separation conditions of gas chromatography are given in Table. 1.

Quantitative analysis is conducted based on the external standard method for CF_4, C_2F_6, C_3F_8, C_3F_6, and CO. For other characteristic decomposition products without standard gas, a manual quantitative peak area integration method was adopted for relative quantitative analysis based on the National Institute of Standards and Technology (NIST14.0) database.

C. TEST METHODS AND STEPS
Normally, gas pressure in medium-voltage (MV) equipment generally lower than 0.20 MPa (absolute pressure) [15], [16]. It was pointed out that the content of C_4F_7N in the gas mixture should not exceed 18% in order to satisfy the minimum operating temperature of $-25°C$ at 0.1-0.2 MPa [8]. In this article, we used gas mixture with 15% C_4F_7N at 0.14 MPa to explore the POF decomposition properties of C_4F_7N-CO_2-O_2 gas mixture under different oxygen contents and temperatures conditions. As shown in Table 2, totally 11 groups of tests were conducted according to the following steps: (1) The gas chamber was cleaned using anhydrous alcohol to remove impurities and then connected. (2) C_4F_7N-CO_2-O_2 gas mixture was filled and then vacuumed for three times to remove gaseous impurities. (3) The relevant POF temperature value was set, then the test was conducted for 12h. The gas in the chamber was collected every 2 hours, followed by the analyses through GC-MS.

TABLE 2. Thermal Decomposition Test Conditions of C_4F_7N-CO_2-O_2 Gas Mixture.

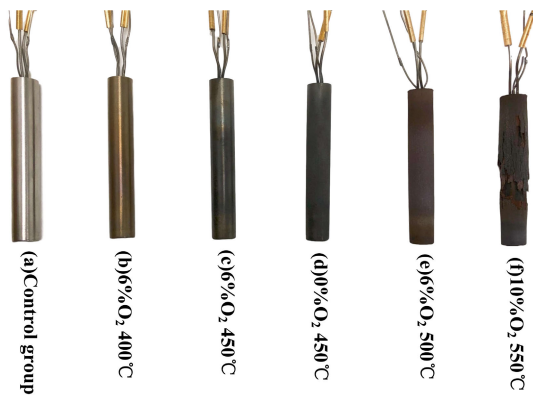| No.	Gas mixture composition	Test temperature (°C)	Pressure (MPa)
1	15%C_4F_7N-85%CO_2-0%O_2	450	0.14
2	15%C_4F_7N-83%CO_2-2%O_2	450	0.14
3	15%C_4F_7N-81%CO_2-4%O_2	450	0.14
4	15%C_4F_7N-79%CO_2-6%O_2	450	0.14
5	15%C_4F_7N-77%CO_2-8%O_2	450	0.14
6	15%C_4F_7N-75%CO_2-10%O_2	450	0.14
7	15%C_4F_7N-79%CO_2-6%O_2	400	0.14
8	15%C_4F_7N-79%CO_2-6%O_2	425	0.14
9	15%C_4F_7N-79%CO_2-6%O_2	475	0.14
10	15%C_4F_7N-79%CO_2-6%O_2	500	0.14
11	15%C_4F_7N-79%CO_2-6%O_2	525	0.14

FIGURE 2. Heating element under different test conditions.

III. RESULTS AND DISCUSSION

A. SURFACE MORPHOLOGY OF HEATING ELEMENT UNDER DIFFERENT TEST CONDITIONS

Figure 2 shows the surface morphology of heating element after 12h POF test under different test conditions. The heating element has been all carbonized at 450°C during the 12h test (shown in Figure 2 (d)). The carbon may originate from the interaction between C_4F_7N and metal heating element. The heating element for 15%C_4F_7N/79%CO_2/6%O_2 gas mixture still shows a certain metallic luster after 12h POF test (shown in Figure 2 (c)), which presumably results from the reaction between O_2 and carbon generates CO_2 and suppresses carbon deposition. Thus, the carbon deposition in GIE using C_4F_7N/CO_2 gas mixture can be inhibited upon the addition of a certain content of O_2.

The heating element for $C_4F_7N/CO_2/O_2$ gas mixture with 10% O_2 was severely corroded under 550°C after test (shown in Figure 2 (f)), which may be ascribed to the oxidation of heating element aggravated by higher O_2 content and temperature. Thus, higher O_2 content and severe POF will cause corrosion of the internal metal components of GIE. The addition amount of O_2 inside the GIE using C_4F_7N/CO_2 gas mixture should not be too high due to the strong oxidation of O_2. The specific addition amount of O_2 will be further explained later combined with the decomposition characteristics of the gas mixture.
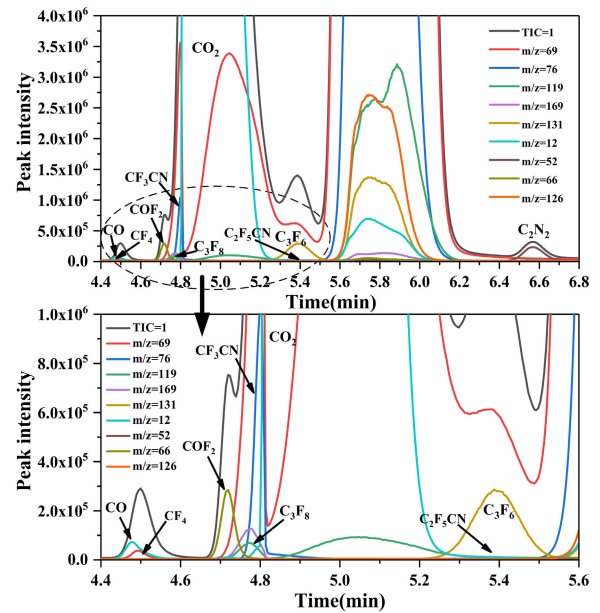

FIGURE 3. Gas chromatogram obtained from the gas collected after the thermal decomposition; (15%C4F7N-6%O2-79%CO2, 0.15MPa, 450°C 12h).

TABLE 3. Mass Charge Ratio of Detected Decomposition Products of C_4F_7N Gas Mixture.

Decomposition by-products	mass charge ratio (m/z)
CO	**12**
CF_4	**69**
C_3F_8	**119**，69，169
C_3F_6	69，**131**，100
COF_2	**66**，50
CF_3CN	**76**，69
C_2F_5CN	76，**126**，69
C_2N_2	**52**

B. MAIN THERMAL DECOMPOSITION PRODUCTS OF C4F7N/CO2/O2 GAS MIXTURE

Figure 3 shows the gas chromatogram of 15%C_4F_7N/6%O_2/ 79%CO_2 gas mixture after 12h POF test (0.14MPa, 450°C). The black curve represents the total ion chromatogram (TIC), the curves of other colors donate the chromatograms of particles with different mass-to-charge ratios (m/z) respectively. The detected mass-to-charge ratios (m/z) of the C_4F_7N gas mixture decomposition products were listed in Table 3.

Obvious characteristic peaks can be observed in the retention time of 4.4-6.8min in Figure 3. According to the compound database in GC/MS, several identified compounds are fluorocarbons (CF_4, C_3F_8, and C_3F_6), oxygenated compounds (CO and CF_2O), and nitrile compounds (CF_3CN, C_2F_5CN, and $(CN)_2$). Literature [6] indicated that the thermal decomposition of C_4F_7N starts at 650°C and generated C_2F_6, COF_2, CF_3CN, C_2F_5CN and CO at 775°C, which is inconsistent with our results. This difference mainly originates from the different test method. Thermal stability test in reference [6] was performed in a tube furnace while the POF physical
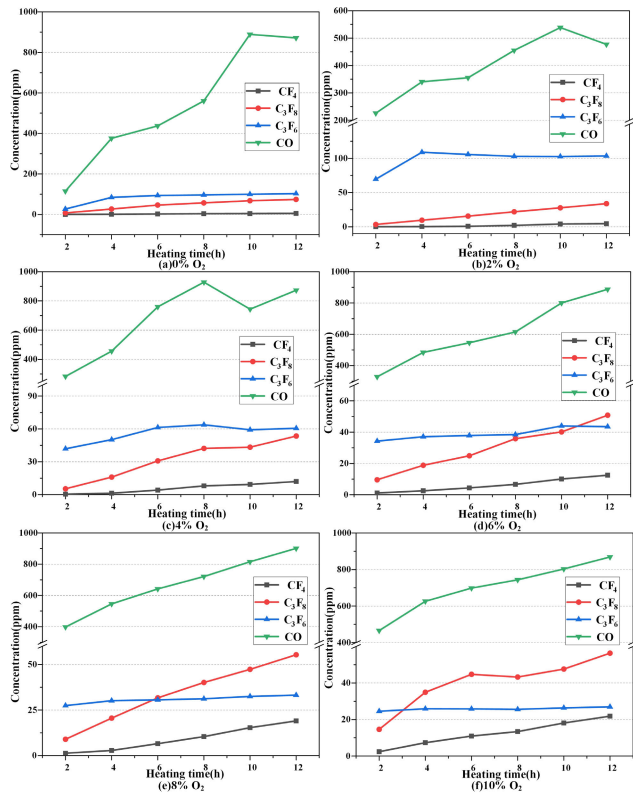
FIGURE 4. The content of CF_4, C_3F_8, C_3F_6 and CO after 450°C overheating tests for $C_4F_7N/CO_2/O_2$ gas mixture with different oxygen content ((a) 0%O_2, (b) 2%O_2, (c) 4%O_2, (d) 6%O_2, (e) 8%O_2, (f) 10%O_2).

defect model is employed to simulate the POF in GIE in this article.

C. INFLUENCE OF OXYGEN ON THE THERMAL DECOMPOSITION PROPERTIES OF $C_4F_7N/CO_2/O_2$ GAS MIXTURE

1) VARIATION FEATURE OF CF_4, C_3F_8 C_3F_6 AND CO

Figure 4 shows yield variation of CF_4, C_3F_8, C_3F_6 and CO after POF test (450°C,12 hours) with different O_2 content. CO, C_3F_6, C_3F_8, CF_4 are the four main by-products when the O_2 content is in the range of 0%-4%. The yields of CO and CF_4 are the respective highest and the lowest among all the by-products. When the O_2 content is higher than 4%, the yield of C_3F_8 is higher than that of C_3F_6. Table 4 displays all possible reaction paths of the $C_4F_7N/CO_2/O_2$ gas mixture under POF test. The main free radicals generated in the decomposition are CF_3, CF_2, CF_2, C_2F_5, C_3F_7, CF, F, C, O and CN (See D1-D14), and most of the decomposition products are generated by recombination of these free radicals (See R1-R14).

According to our previous study on the discharge decomposition characteristics of $C_4F_7N/CO_2/O_2$ gas mixture, the yield of CF_4 is the highest, followed by CO [12]. The yield of these two products is much lower under POF decomposition. The main origin for this difference may be that the temperature can reach 3000K in the center of the discharge [17] and the high-energy arc instantly breaks the chemical bonds of C_4F_7N molecules in the gas mixture. A large number

TABLE 4. The Possible Dissociation and Recombination Pathways of $C_4F_7N/CO_2/O_2$ Gas Mixture.

Path	Decomposition reaction	Path	Recombination reaction
D1	$C_4F_7N \rightarrow (CF_3)_2CF+CN$	R1	$CF_3+F \rightarrow CF_4$
D2	$C_4F_7N \rightarrow (CF_3)_2C(CN)+F$	R2	$CF_2+CF_2 \rightarrow C_2F_4$
D3	$C_4F_7N \rightarrow CF_3CFCN+CF_3$	R3	$(CF_3)_2CF+F \rightarrow C_3F_8$
D4	$C_4F_7N \rightarrow CF_3CF_2CFCN+F$	R4	$CF_2=C-CF_3+F \rightarrow C_3F_6$
D5	$(CF_3)_2CF \rightarrow (CF_3)_2C+F$	R5	$CF_3+CN \rightarrow CF_3CN$
D6	$(CF_3)_2C \rightarrow CF_2=C-CF_3+F$	R6	$C_2F_5+CN \rightarrow C_2F_5CN$
D7	$CF_2=CF-CF_3 \rightarrow CF_2=CF+CF_3$	R7	$CN+CN \rightarrow C_2N_2$
D8	$CF_3CFCN \rightarrow CFCN+CF_3$	R8	$CF_2+O \rightarrow COF_2$
D9	$CF_3CFCN \rightarrow CN+CF_3CF$	R9	$CF_3+O \rightarrow COF_2+F$
D10	$CF_3CF \rightarrow C-CF_3+F$	R10	$C_2F_4+O_2 \rightarrow 2COF_2$
D11	$CF_3 \rightarrow CF_2+F$	R11	$CF+F+O \rightarrow COF_2$
D12	$CF_2 \rightarrow CF+F$	R12	$2C+O_2 \rightarrow 2CO$
D13	$CO_2 \rightarrow CO+O$	R13	$C+O_2 \rightarrow CO_2$
D14	$O_2 \rightarrow O+O$	R14	$2CO+O_2 \rightarrow 2CO_2$

of particle fragments are generated, and complex chemical reactions occur between them. The formation of CF_4 requires CF_3 and F particles, which are more likely to be generated than other particles based on density functional theory (DFT) calculations [18]. Thus, the yield of CF_4 is the highest in discharge decomposition. For POF, the test temperature ranges from 400°C to 525°C and the released thermal energy is lower. Therefore, the yield of CF_4 and CO is much lower. Actually, the wave function of the C_4F_7N front molecular orbital is mainly distributed on the carbon atoms connected to the CN group and its adjacent carbon atoms. The high reactivity of CN group probably results in the interaction between C_4F_7N molecules and metallic heating elements under high temperature to generate C_3F_7 and CN particles (shown in Table 4 (D1)). C_3F_7 particles could combine with F particles to form C_3F_8 (shown in Table 4 (R3)) or be decomposed to generate C_3F_6, which is also confirmed by the previous research on the compatibility between C_4F_7N/CO_2 and metal [19]. The gas by-product C_3F_6 was firstly detected at 220°C during the gas-solid interface reaction [19]. Therefore, the yield of C_3F_6 and C_3F_8 is higher than CF_4 under POF decomposition conditions.

As shown in Table 4, the generation of CO mainly originates from the following aspects: (1) The combination of activated C in stainless steel of heating element and O. (2) The decomposition of CO_2. (3) The reduction reaction of CO_2 and C particles at high temperature. Therefore, the content of CO is found to be highest in the POF decomposition experiments.

In addition, it can be found that yield of CF_4 and C_3F_8 increase as overheating time aging. The content of CF_4 reached 21.84 ppm when 10% oxygen was added and. The maximum yield of C_3F_8 is 74.38ppm (0%O_2,12h). The yield of C_3F_6 begins to be unchanged after 6 h POF test and the maximum increment does not exceed 3.5 ppm, indicating that the yield of C_3F_6 saturates with POF time. The smaller change trend of C_3F_6 can be found with higher O_2 content, indicating that the addition of oxygen counts against the generation of C_3F_6. For example, the difference between the maximum and the minimum value of C_3F_6 during the 12h POF test is 76.39ppm (0% O_2), 33.86ppm (2% O_2), 18.77ppm (4% O_2), 9.22ppm (6% O_2), 5.74ppm (8% O_2) and 2.42ppm (10% O_2). The yield of CO exhibited obvious

increasing trend with the POF time and its maximum yield reached 928.26 ppm(4%O_2,12h).

The POF in GIE starts with a low-energy latent fault, which may develop into a serious high-energy fault if corresponding measures are not performed in time. Actually, it is difficult to make a correct judgment of the fault severity based on the yield of the decomposition products, thus the gas production rate must be considered. The effective gas production rate can directly reflect the magnitude of energy consumed by the fault, the severity and development process of the fault [13]. As defined in equation (1), R_i is the absolute gas production rate, C_{i1} and C_{i2} denote the contents (ppm or peak area) of component i measured at the first and second times respectively, Δt represents the time interval between the two tests.

$$R_i = \frac{C_{i1} - C_{i2}}{\Delta t} \quad (1)$$

In this article, the statistically significant effective gas production rate R_{RMS} was used to describe the change trend of different characteristic components. In equation (2), R_{ij} is the absolute gas production rate ($j = 2,4,6,8,10,12$) of the decomposition component i at the jth hour, and n is the number of gas samples.

$$R_{RMS} = \sqrt{\frac{\sum_{j-1}^{n} R_{ij}^2}{n}} \quad (2)$$

Figure 5(a) shows the yield and effective formation rate of CF_4 under various O_2 contents. The yield of CF_4 reaches 5.3 ppm, 4.58 ppm and 11.17 ppm at 12 h when 0% O_2, 2% O_2 and 4% O_2 is added to C_4F_7N/CO_2 gas mixture respectively. The addition of 2% O_2 to C_4F_7N/CO_2 gas mixture could slightly reduce the yield of CF_4, the effective formation rate remains basically unchanged. The stable yield and effective formation rate of CF_4 can be maintained when 4%~6% oxygen is added and start to increase sharply when O_2 is higher than 6%. Positive correlation between CF_4 yield with O_2 content indicates that the decomposition of C_4F_7N is accelerated upon the addition of O_2.

The content of C_3F_8 in the C_4F_7N/CO_2 gas mixture reached 74.38ppm after 12h POF test, while this value is 33.82ppm for the gas mixture containing 2% O_2 (as shown in Figure 5(b)). The yield and effective formation rate of C_3F_8 remain stable for the gas mixture with 4%-8% O_2, which began to increase when the oxygen content exceeds 8%. The content of C_3F_8 is 56.32ppm (12h) when 10% O_2 is added to the C_4F_7N/CO_2 gas mixture, while this value is still lower than that of C_4F_7N/CO_2 gas mixture. This implies that the addition of O_2 inhibits the generation of C_3F_8.

Figure 5(c) demonstrated the change trend of yield and effective formation rate of C_3F_6 under different O_2 content conditions at 450°C. The yield of C_3F_6 increased from 26.69 ppm (2h), 84.2 ppm (4h) to 69.65 ppm (2h), 108.98 ppm (4h) when 2% O_2 was added in the C_4F_7N/CO_2 gas mixture, its content keeps stable at 6-12 h. The yield and effective information rate of C_3F_6 decrease sharply when the oxygen content was higher than 2%, which may be due to the oxidization of C_3F_6 considering the unsaturated C=C bond.

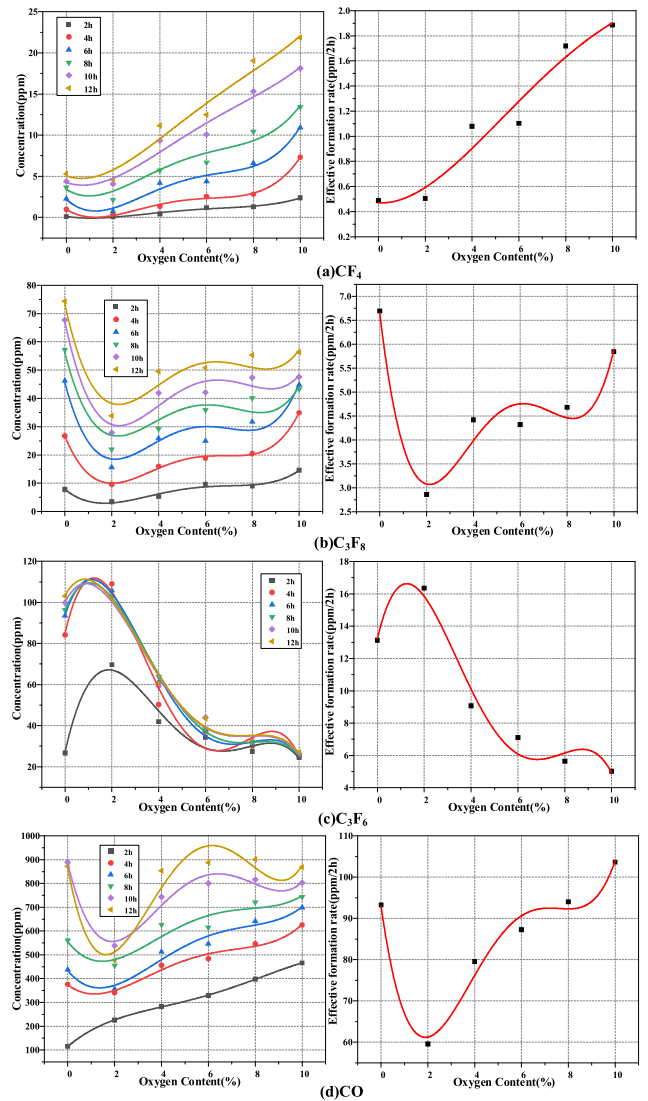The yield of CO decreased from 871.61 ppm (12h) to 477.25 ppm (12h) when 2% O_2 was added in the C_4F_7N/CO_2

FIGURE 5. The yield and effective formation rate of products under different O2 content conditions. (a) CF_4, (b) C_3F_8, (c) C_3F_6, (d) CO.

gas mixture, exhibiting a saturated growth trend at 4%~10% O_2 conditions (as shown in Figure 5(d)). CO is mainly generated from the decomposition of CO_2 in the C_4F_7N/CO_2 gas mixture. In addition, the reaction between the C particles in the stainless-steel heating element and O_2 may occur at high temperatures to generate CO with higher O_2 content.

2) VARIATION FEATURE OF COF_2, CF_3CN, C_2F_5CN AND C_2N_2

Figure 6(a) shows the yield and effective formation rate of COF_2 under different O_2 contents at 450°C. The yield and effective formation rate of COF_2 both decreased when 2% O_2 was added and then increased at 4%-10% O_2 conditions. The yield of COF_2 started to increase significantly when oxygen content exceeded 8%. The addition of O_2 contributes to the decomposition of C_4F_7N, resulting in the generation of CF_x particles, which then could react with O_2 to generate COF_2.

The yield and effective formation rate of CF_3CN, C_2F_5CN decreased sharply when 2% O_2 was added to C_4F_7N/CO_2 gas
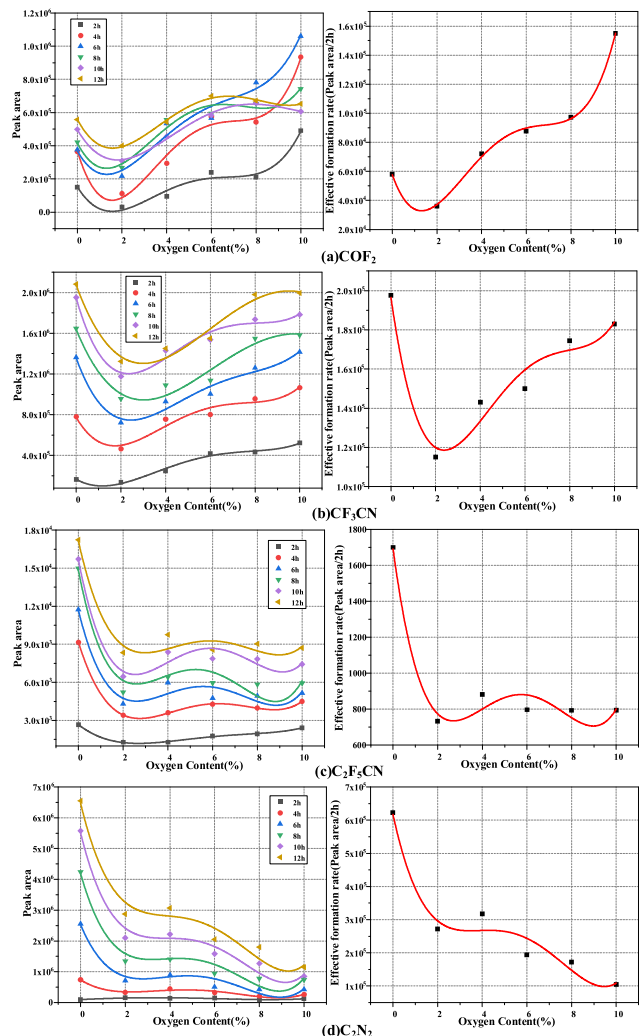
FIGURE 6. The yield and effective formation rate of products under different O_2 content conditions. (a)COF_2, (b)CF_3CN, (c)C_2F_5 CN, (d)C_2N_2.

mixture and increased when O_2 content was higher than 2% (Figure 6 (b), (c)). CF_3CN mainly comes from the recombination of CF_3 and CN particles and C_2F_5CN mainly arises from the recombination of C_2F_5 and CN particles. Higher oxygen content could aggravate the decomposition of C_4F_7N, resulting in the massive formation of CN particles, thus the yield of CF_3CN increases sharply and the yield of C_2F_5CN remain basically unchanged when the oxygen content is higher than 6%. In addition, the yield and effective formation rate of C_2N_2 decreased upon the addition of oxygen (Figure 6 (d)).

D. INFLUENCE OF TEMPERATURE ON THE THERMAL DECOMPOSITION PROPERTIES OF C_4F_7N/CO_2/O_2 GAS MIXTURE

1) VARIATION FEATURE OF CF_4, C_3F_8, C_3F_6 AND CO

Figure 7 shows the yield change of CF_4, C_3F_8, C_3F_6 and CO in 15%C_4F_7N/79%CO_2/6%O_2 gas mixture after 12h POF test under various temperature conditions. The yield of CO is the highest among all decomposition products at 400°C-525°C, followed by C_3F_6 and C_3F_8. The yield of CF_4
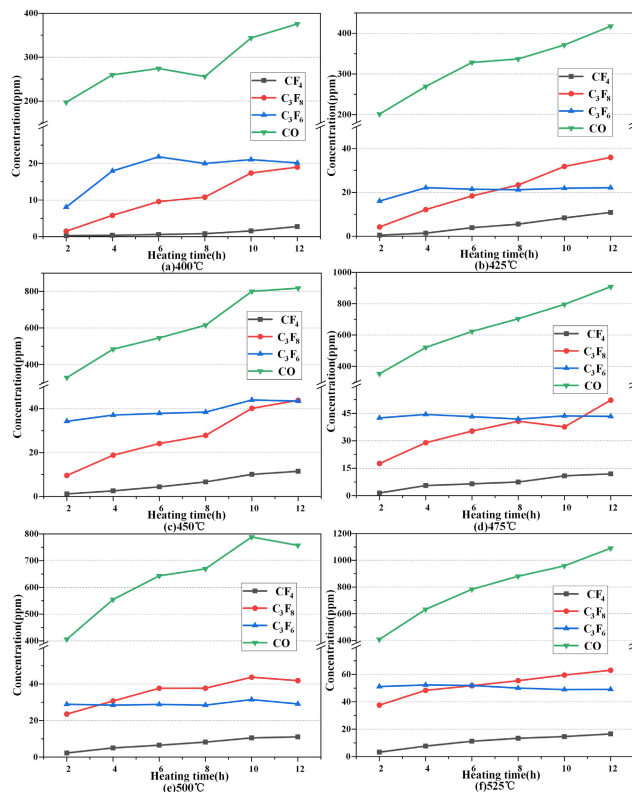

FIGURE 7. The yield of CF_4, C_3F_8, C_3F_6 and CO after overheating test for C_4F_7N/CO_2/O_2 gas with different temperature ((a) 400°C, (b) 425°C, (c)450°C, (d)475°C, (e) 500°C, (f) 525°C).

is much lower than other products. The variation trend of main decomposition products with overheating time at different temperatures can be observed from Figure 7. At 525°C, the yield of CF_4 is 3.22ppm (2h), 16.56ppm (12h); the yield of C_3F_8 is 37.53ppm (2h). 63.03ppm (12h); the yield of C_3F_6 is 51.13ppm (2h), 49.09 (12h); the yield of CO is 408.07ppm (2h), 1092.27ppm (12h). It can be noted that the yield of C_3F_6 is almost unchanged with the increased overheating time under higher temperature, while the yield of the remaining products changes obviously with the overheating time. Furthermore, the higher temperature can result in the smaller variation trend of C_3F_6 content with overheating time.

Figure 8(a) shows the yield and effective formation rate of CF_4 under different temperature conditions. The content of CF_4 increases sharply at 400-425°C and 500-525°C, maintaining stable at 425-500°C. The initial temperature for CF_4 generation is about 400°C and its content has no clear distinction at different temperatures. The yield and effective formation rate of C_3F_8 shows positive correlation with temperature in the range of 400-525°C and its content is lower than 10ppm after 12h POF tests (as shown in Figure 8 (b)).

The yield of C_3F_6 increase with temperature at 400-475°C and the highest content reaches 43.34ppm (12h, 475 °C). Then its content decreased to 27 ppm at 500°C and increased again at 525°C (as shown in Figure 8 (c)). As mentioned above, part of C_3F_6 is generated by the interaction between C_4F_7N and the metal heating element. The metal heating element is destroyed when the temperature is boosted up to 500°C, thus leading to the decreased yield of C_3F_6. The
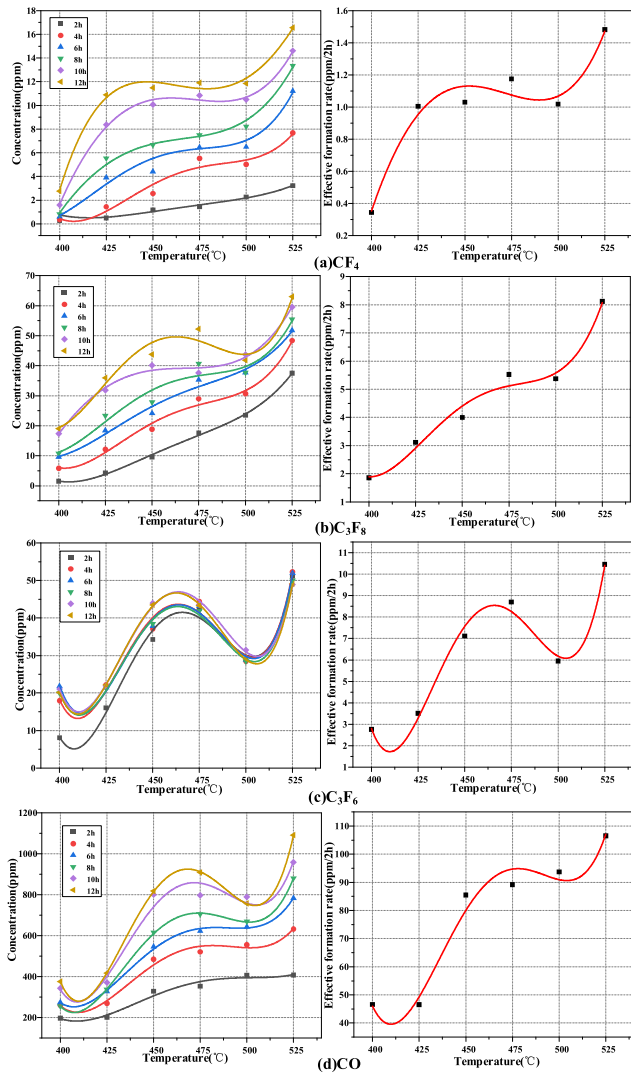
FIGURE 8. The yield and effective formation rate of products under different temperature conditions. (a) CF_4, (b) C_3F_8, (c) C_3F_6, (d) CO.
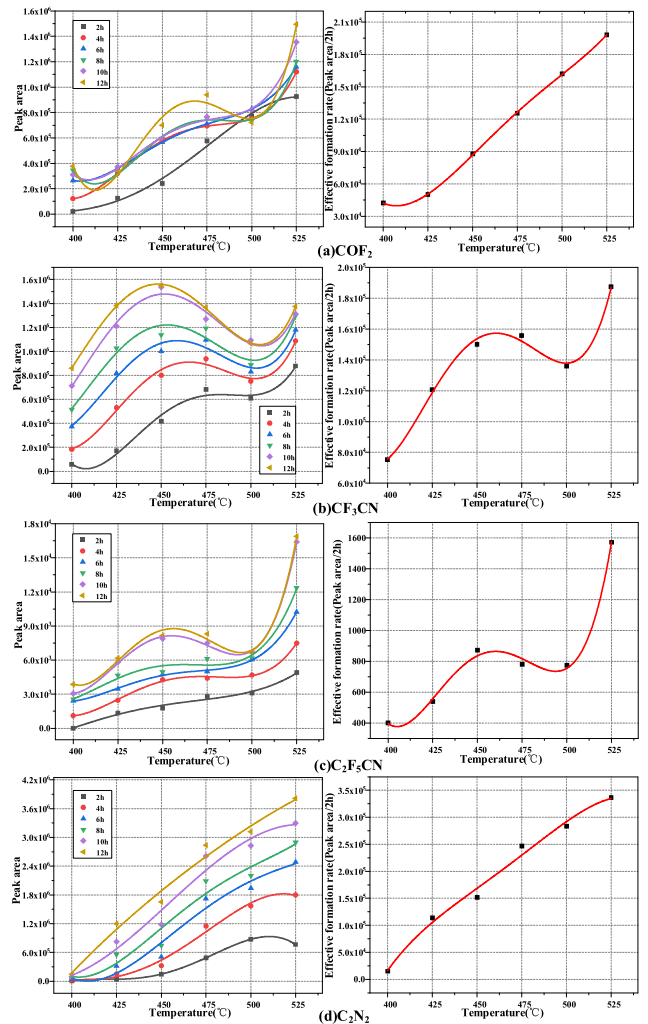

FIGURE 9. The yield and effective formation rate of products under different temperature conditions. (a)COF2, (b)CF3CN, (c)C2F5CN, (d)C2N2.

increase of C_3F_6 at 525°C may originates from the severe thermal decomposition of C_4F_7N.

In addition, the yield and effective formation rate of CO is stable at 400-425°C, which is then increased sharply at 425°C-450°C. And a saturated growth trend was found at 450-525°C. Thus, the generation of CO mainly starts at 425°C.

2) VARIATION FEATURE OF COF_2, CF_3CN, C_2F_5CN AND C_2N_2

Figure 9(a) shows the change trend of yield and effective formation rate of COF_2 under different temperature conditions. The generation rate of COF_2 shows linear increase trend with temperature, which can be used as a characteristic product to examine the severity of POF.

The yield and effective formation rate of CF_3CN, C_2F_5CN demonstrates similar change trend with temperature (as shown in Figure 9 (b)-(c)). Their content increase with temperature in the range of 400°C-450°C and trends to be saturated at 450°C-500°C. The content of CF_3CN, C_2F_5CN

increase sharply when the temperature exceeds 500°C. Therefore, CF_3CN and C_2F_5CN can be utilized as characteristic product to reveal the severe POF in GIE. In addition, the effective formation rate of C_2N_2 increases linearly with temperature basically, thus this component can also be used as a characteristic product to characterize the severity of POF in $C_4F_7N/CO_2/O_2$ gas mixture based GIE.

E. DISCUSSION

According to the above test results, it can be found that adding a certain amount of O_2 to the C_4F_7N/CO_2 gas mixture have a greater impact on the thermal stability of the gas mixture. The yield of CF_4, C_3F_8, CO, COF_2, CF_3CN, C_2F_5CN, C_2N_2 is reduced to varying degrees at 450°C when 2% O_2 is added to the C_4F_7N/CO_2 gas mixture. Literature [12] points out that the yield of the above decomposition products generated by discharge decomposition of $C_4F_7N/CO_2/O_2$ gas mixture with 2% O_2 also decreased, indicating that addition of certain amount of O_2 could inhibit the decomposition of C_4F_7N under POF and discharge conditions.

TABLE 5. The Properties of the Pure Gas and the Decomposition Products.

Pure gas and by-products	Global Warming Potential (GWP)	Toxicity (LC_{50}) (ppm)	Dielectric strength (relative to SF_6)
C_4F_7N	2100	10000-15000(rat,4h)	2.2
CF_4	6300	20000(rat,4h)	0.42
C_3F_8	7000	90000(rat,4h)	0.88
C_3F_6	8000	3060(rat,4h)	1.02
CO	1~3	1880(rat,4h)	0.4
COF_2	-	180(rat,4h)	-
CF_3CN	-	250(rat,4h)	1.34-1.40
C_2F_5CN	-	2730(rat,4h)	1.80-1.85
C_2N_2	-	175(rat,4h)	-

When O_2 content is higher than 2%, the yields of other products increased except C_3F_6 and C_2N_2, and a sharply increase trend of C_3F_8 and COF_2 was observed when the O_2 content is higher than 8%, indicating that excessive oxygen could accelerate the decomposition of C_4F_7N/CO_2 gas mixture. According to Table 5, C_2N_2, COF_2 and CF_3CN demonstrates the highest toxicity among all by-products with the LC50 (rat,4h) of 175 ppm, 180 ppm, 250 ppm respectively. It was also found that the yield of CF_3CN and COF_2 increases sharply when the oxygen content is higher than 6% and 8%. Furthermore, literature [12] demonstrates that the dielectric strength of $C_4F_7N/CO_2/O_2$ gas mixture with 2%, 4%, 6%, 8% and 10% oxygen is increased by 4.85%, 6.49%, 7.70%, 3.21% and 2.74% compared to C_4F_7N/CO_2 and the insulation performance starts to decrease when the O_2 content is higher than 6%, indicating the oxygen addition should not exceed 6%. The yield of C_2N_2 gradually decreases with the content of O_2, implying the O_2 content should not be too low due to the highest toxicity of C_2N_2. Furthermore, it was pointed out that that addition of 5% O_2 to C_4F_7N/CO_2 gas mixture could improve the electrical endurance of the circuit breaker by inhibiting the generation of gaseous and solid decomposition products [10]. Therefore, addition of 4-6% O_2 to the C_4F_7N/CO_2 gas mixture is ideal considering the insulation performance, arc extinction, decomposition characteristics and safety.

As mentioned above, the POF temperature could also exhibit a greater impact on the thermal stability and decomposition characteristics of $C_4F_7N/CO_2/O_2$ gas mixture. The yield and effective formation rate of CO, COF_2, CF_4, C_3F_8, C_3F_6, CF_3CN, C_2F_5CN, C_2N_2 increase with temperature in the range of 400°C $\sim$ 525°C. Among them, the effective formation rate of COF_2 and C_2N_2 shows a strong positive linear correlation with POF temperature, which can be used as characteristic products to examine the POF severity of $C_4F_7N/CO_2/O_2$ gas mixture based GIE. In addition, the yield and effective formation rate of C_2F_5CN increased sharply when the POF temperature exceeds 500°. Thus, C_2F_5CN can be utilized as symbolic decomposition product to be as an indicator of the severe POF in GIE.

IV. CONCLUSION

In this article, we explored the thermal decomposition characteristics of $C_4F_7N/CO_2/O_2$ gas mixture under different O_2 content and temperature conditions. The following useful conclusions can be obtained,

(1) The main decomposition products of $C_4F_7N/CO_2/O_2$ gas mixture includes CF_4, C_3F_8, C_3F_6, CO, COF_2, CF_3CN, C_2F_5CN, C_2N_2 under POF. Addition of 2% O_2 in C_4F_7N/CO_2 gas mixture results in the yield increase of C_3F_6 and decrease of other by-products. The content of CF_4, C_3F_8, CO, COF_2 and CF_3CN increases under the condition of 4%-10% O_2.

(2) The yield and effective formation rate of CF_4, C_3F_8, C_3F_6, CF_3CN and C_2F_5CN increase at 400°C-525°C. The effective formation rate of both COF_2 and C_2N_2 show a strong positive correlation with POF temperature.

(3) It is recommended to add 4-6% O_2 in C_4F_7N/CO_2 gas mixture for MV engineering application. COF_2, C_2N_2 and C_2F_5CN can be utilized as characteristic products to evaluate the POF severity of $C_4F_7N/CO_2/O_2$ gas mixture based GIE.

REFERENCES

[1] F. Zeng, S. Wu, Z. Lei, C. Li, J. Tang, Q. Yao, and Y. Miao, "SF₆ fault decomposition feature component extraction and triangle fault diagnosis method," *IEEE Trans. Dielectr. Electr. Insul.*, vol. 27, no. 2, pp. 581–589, Apr. 2020.

[2] S. Xiao, B. Gao, X. Pang, X. Zhang, Y. Li, S. Tian, J. Tang, and Y. Luo, "The sensitivity of C_4F_7N to electric field and its influence to environment-friendly insulating gas mixture C_4F_7N/CO_2," *J. Phys. D, Appl. Phys.*, vol. 54, no. 5, Feb. 2021, Art. no. 055501, doi: 10.1088/1361-6463/abbc97.

[3] Y. Li, X. Zhang, S. Tian, S. Xiao, Y. Li, and D. Chen, "Insight into the decomposition mechanism of $C_6F_{12}O$-CO_2 gas mixture," *Chem. Eng. J.*, vol. 360, pp. 929–940, Mar. 2019.

[4] X. Ai, Y. Tu, Y. Zhang, G. Chen, Z. Yuan, C. Wang, X. Yan, and W. Liu, "The effect of electrode surface roughness on the breakdown characteristics of C_3F_7CN/CO_2 gas mixtures," *Int. J. Electr. Power Energy Syst.*, vol. 118, Jun. 2020, Art. no. 105751.

[5] M. Rabie and C. M. Franck, "Assessment of eco-friendly gases for electrical insulation to replace the most potent industrial greenhouse gas SF₆," *Environ. Sci. Technol.*, vol. 52, no. 2, pp. 369–380, Jan. 2018.

[6] X. Zhang, Y. Wang, Y. Li, Y. Li, F. Ye, S. Tian, D. Chen, S. Xiao, and J. Tang, "Thermal compatibility properties of $C_6F_{12}O$-air gas mixture with metal materials," *AIP Adv.*, vol. 9, no. 12, Dec. 2019, Art. no. 125024.

[7] Y. Kieffel, "Characteristics of g³-an alternative to SF₆," in *Proc. IEEE Int. Conf. Dielectr.*, Jul. 2016, pp. 880–884.

[8] Y. Kieffel, T. Irwin, P. Ponchon, and J. Owens, "Green gas to replace SF₆ in electrical grids," *IEEE Power Energy Mag.*, vol. 14, no. 2, pp. 32–39, Mar. 2016.

[9] X. Zhang, Q. Chen, J. Zhang, Y. Li, S. Xiao, R. Zhuo, and J. Tang, "Experimental study on power frequency breakdown characteristics of C_4F_7N/CO_2 gas mixture under quasi-homogeneous electric field," *IEEE Access*, vol. 7, pp. 19100–191087, 2019.

[10] A. Chachereau, A. Hösl, and C. M. Franck, "Electrical insulation properties of the perfluoronitrile C_4F_7N," *J. Phys. D, Appl. Phys.*, vol. 51, no. 49, Dec. 2018, Art. no. 495201.

[11] F. Meyer, P. Huguenot, and Y. Kieffell, "Application of fluoronitrile/CO_2/O_2 mixtures in high voltage products to lower the environmental footprint," CIGRE, Paris, France, Tech. Rep. D1-201, 2018.

[12] C. Lindner and D. Gautsch, "Application of a fluoronitrile gas in a 123 kV GIS pilot substation," CIGRE, Paris, France, Tech. Rep. B3-146, 2018.

[13] Y. Li, X. Zhang, F. Ye, D. Chen, S. Tian, and Z. Cui, "Influence regularity of O_2 on dielectric and decomposition properties of C_4F_7N–CO_2–O_2 gas mixture for medium-voltage equipment," *High Voltage*, vol. 5, no. 3, pp. 256–263, Jun. 2020.

[14] F. Zeng, J. Tang, Q. Fan, J. Pan, X. Zhang, Q. Yao, and J. He, "Decomposition characteristics of SF₆ under thermal fault for temperatures below 400°C," *IEEE Trans. Dielectr. Electr. Insul.*, vol. 21, no. 3, pp. 995–1004, Jun. 2014.

[15] Y. Li, X. Zhang, J. Zhang, C. Xie, X. Shao, Z. Wang, D. Chen, and S. Xiao, "Study on the thermal decomposition characteristics of C_4F_7N–CO_2 mixture as eco-friendly gas-insulating medium," *High Voltage*, vol. 5, no. 1, pp. 46–52, Feb. 2020.

[16] C. Preve, D. Piccoz, and R. Maladen, "Validation method and comparison of SF_6 alternative gases," CIGRE, Paris, France, Tech. Rep. D1-205, 2016.

[17] C. Preve, G. Lahaye, M. Richaud, R. Maladen, T. Penelon, and S. Galas, "Hazard study of medium-voltage switchgear with SF_6 alternative gas in electrical room," *CIRED-Open Access Proc. J.*, vol. 2017, no. 1, pp. 198–201, Oct. 2017.

[18] Y. Fu, A. Yang, X. Wang, A. B. Murphy, X. Li, D. Liu, Y. Wu, and M. Rong, "Theoretical study of the neutral decomposition of SF_6 in the presence of H_2O and O_2 in discharges in power equipment," *J. Phys. D, Appl. Phys.*, vol. 49, no. 38, Sep. 2016, Art. no. 385203.

[19] B. Zhang, C. Li, J. Xiong, Z. Zhang, X. Li, and Y. Deng, "Decomposition characteristics of C_4F_7N/CO_2 mixture under AC discharge breakdown," *AIP Adv.*, vol. 9, no. 11, Nov. 2019, Art. no. 115212.

[20] Y. Li, X. Zhang, J. Zhang, Q. Chen, Y. Li, S. Xiao, and J. Tang, "Thermal compatibility between perfluoroisobutyronitrile-CO_2 gas mixture with copper and aluminum switchgear," *IEEE Access*, vol. 7, pp. 19792–19800, 2019.

[21] Y. Li, X. Zhang, J. Zhang, S. Xiao, B. Xie, D. Chen, Y. Gao, and J. Tang, "Assessment on the toxicity and application risk of C_4F_7N: A new SF_6 alternative gas," *J. Hazardous Mater.*, vol. 368, pp. 653–660, Apr. 2019.

XIANG SUN was born in Jinhua, Zhejiang, China, in 1979. He received the master's degree in electrical engineering from Xi'an Jiaotong University, Xi'an, China. He is currently an Engineer with the State Grid Zhejiang Electric Power Research Institute. His research interest includes high-voltage equipment online monitoring.
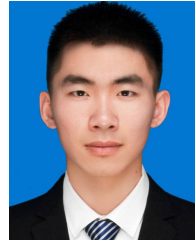
PENG WU was born in Longyan, Fujian, China, in 1996. He received the bachelor's degree in electrical engineering from Fuzhou University, Fuzhou, China. He is currently pursuing the master's degree with the School of Electrical Engineering and Automation, Wuhan University. His research interests include the alternative gas of SF_6 and new nano-sensor for gas detection.

FANCHAO YE was born in Honghu, Hubei, China, in 1993. He received the master's degree in electrical engineering from the Hubei University of Technology, Wuhan, China. He is currently pursuing the Ph.D. degree with the School of Electric Engineering, Wuhan University. His research interests include the alternative gas of SF_6 and the fault diagnosis of high voltage electrical insulation equipment.

SONG XIAO (Member, IEEE) was born in Zhangjiakou, Hebei, China, in 1988. He received the B.S. and Ph.D. degrees in electrical engineering from Chongqing University, Chongqing, China, and the Ph.D. degree in plasma engineering from the Universit'e de Toulouse, Toulouse, France. He is currently an Associate Professor with the School of Electrical Engineering and Automation, Wuhan University. His research interests include partial discharge online monitoring and gas substituting SF_6.

XIAOXING ZHANG was born in Qianjiang, Hubei, China, in 1972. He received the bachelor's and master's degrees from the Hubei University of Technology and the Ph.D. degree from Chongqing University. He is currently a Professor of the School of Electric Engineering, Wuhan University. He is involved in the online monitoring and fault diagnosis of high voltage electrical insulation equipment, alternative gases of SF_6, the decomposition mechanism of insulating gas SF_6, and new nano-sensor.

JU TANG (Member, IEEE) was born in Pengxi, Sichuan, China, in 1960. He received the B.Sc. degree from Xi'an Jiaotong University, Xi'an, China, and the M.Sc. and Ph.D. degrees from Chongqing University, Chongqing, China. He is currently a Professor with the School of Electrical Engineering and Automation, Wuhan University, and also the Chief Scientist presiding over a National Basic Research Program of China (973 Program). He is involved in high-voltage equipment online monitoring, fault diagnosis, signal processing, simulation analysis, and pattern recognition.

CHENG XIE (Member, IEEE) was born in Hangzhou, Zhejiang, China, in 1988. He received the master's degree in electrical engineering from Xi'an Jiaotong University, Xi'an, China. He is currently an Engineer with the State Grid Zhejiang Electric Power Research Institute. His research interest includes the fault diagnosis of high voltage electrical insulation equipment.

YI LI (Graduate Student Member, IEEE) was born in Shangluo, Shanxi, China, in 1994. He received the bachelor's degree in electrical engineering from Wuhan University, Wuhan, China, where he is currently pursuing the Ph.D. degree with the School of Electrical Engineering and Automation. His research interests include the alternative gas of SF_6 and fault diagnosis of high voltage electrical insulation equipment.

• • •